2025 47th Annual International Conference of the IEEE Engineering in Medicine and Biology Society (EMBC) | 979-8-3315-8618-8/25/$31.00 ©2025 Authors | DOI: 10.1109/EMBC58623.2025.11254514

High-Density MEA Reveals Distinct Sharp-Wave Ripple Network Dynamics Across Induction Methods in the Hippocampus

Shahrukh Khanzada, Xin Hu, Brett Addison Emery, Hayder Amin*, *Member, IEEE*

***Abstract*—Learning and memory are fundamental brain functions governed by rhythmic oscillatory activity, which synchronizes neural communication and modulates network dynamics. Distinct oscillatory patterns—theta (θ), beta (β), gamma (γ), and sharp wave-ripples (SWR)—coordinate neural ensemble activity, particularly in the hippocampal CA1-CA3 regions, where they play a crucial role in learning and memory. Understanding the mechanisms underlying SWR generation is crucial, as these oscillations play a fundamental role in memory consolidation, synaptic plasticity, and cognitive function. Unlike previous small-scale studies that relied on limited electrode coverage, our approach leverages high-density microelectrode arrays (HD-MEAs) to capture SWRs across large-scale hippocampal networks. This enables a direct comparison of how different induction methods influence network-wide dynamics, rather than focusing on isolated neuronal activity. By quantitatively assessing spatiotemporal propagation, frequency distributions, and ensemble synchronization, we aim to determine whether experimentally evoked SWRs truly replicate the functional characteristics of their spontaneous counterparts or introduce distinct network properties. Our findings provide a critical foundation for interpreting SWR activity in both physiological and experimental settings, offering novel insights into large-scale neural dynamics and their implications for memory-related processes and therapeutic interventions.**

I. Introduction

The ability to encode, store, and retrieve memories is a fundamental function of the brain, supported by large-scale network activity spanning multiple regions. Within the hippocampus, a crucial structure for spatial navigation and episodic memory, synchronized neuronal activity enables efficient information processing [1], [2]. Among the various oscillatory patterns governing hippocampal function, sharp wave-ripples (SWRs) play a central role in consolidating and transferring memories. These high-frequency spontaneous events emerge primarily in the CA3 region and propagate to CA1, facilitating the replay of neural sequences critical for learning [3]. Despite their importance, the mechanistic diversity in SWR generation and modulation remains an open question, particularly regarding how experimental induction methods compare to naturally occurring SWRs. Oscillatory dynamics in the brain are diverse and vary across cognitive states. Theta (5–12 Hz) rhythms dominate during active exploration and facilitate synaptic plasticity, whereas beta (13–30 Hz) and gamma (30–100 Hz) oscillations support attention, sensory integration, and cognitive control [4]. In contrast, SWRs (~120–250 Hz) occur predominantly during sleep and immobility, serving as a mechanism for experience-dependent memory consolidation [5]. Traditionally, these events have been studied in their spontaneous form, but alternative approaches—such as electrical stimulation and pharmacological modulation—allow us to induce similar activity patterns under controlled experimental conditions [6]. The coordination of these rhythms ensures efficient neural computation, yet most studies have focused on SWRs in isolated small-scale recordings [7], limiting our understanding of their large-scale network effects.

Traditional techniques such as patch-clamp electrophysiology and low-density microelectrode arrays (MEAs) provide sufficient temporal precision but lack the spatial resolution required to capture hippocampal-wide synchronization. Large-scale high-density microelectrode arrays (HD-MEAs) overcome this limitation, enabling simultaneous recordings across thousands of sites [8], [9], [10]. This advancement allows for the direct comparison of spontaneous, electrically evoked, and pharmacologically induced SWRs to determine whether experimental manipulations faithfully replicate the functional properties of natural SWRs.

In this study, we leverage HD-MEA technology to investigate the network-level properties of SWRs induced through electrical stimulation and pharmacological agents (Increase potassium (K^+) ions, and 4-aminopyridine) and compare them with their spontaneous counterparts. Our results reveal key differences in spatiotemporal propagation, spectral composition, and neuronal recruitment, providing new insights into how different induction methods modulate hippocampal network activity. This study establishes a quantitative framework for evaluating SWR dynamics, offering implications for both fundamental neuroscience and translational applications in cognitive enhancement and neuromodulation therapies.

II. Materials and Methods

A. HD-MEA Acquisition

Large-scale HD-MEA chip recordings were performed using a customized acquisition system (3Brain AG, Switzerland). HD-MEA chips are composed of 4096 recording electrodes with a 42-µm pitch size to compose an active sensing area of ~7 mm^2. The on-chip amplification circuit allows for 1 Hz–5 kHz band-pass filtering, conferred by a global gain of 60 dB, allowing precise recording of both slow and fast oscillatory activity. This setup allows us to record

Research supported from basic institutional funds (DZNE) and the ERANET-NEURON (ResiPreS). S. Khanzada, X. Hu, B.A. Emery, and H. Amin are with the Biohybrid Neuroelectronics Laboratory (BIONICS) at the German Center for Neurodegenerative Diseases (DZNE), Tatzberg 41, 01307 Dresden, Germany *Corresponding author (Tel:+49351210463602 - E-mail hayder.amin@dzne.de).

SWR activity with unparalleled spatiotemporal resolution, making it ideal for comparing different induction methods.

B. Hippocampal Acute Slice Preparation

All experiments and animal procedures were performed following the applicable European and national regulations (Tierschutzgesetz) and were approved by the local authority (Landesdirektion Sachsen; 25–5131/476/14). Acute, horizontal 300 µm thick hippocampal-cortical slices were obtained from 12-week-old C57BL/6J mice (Charles River Laboratories, Germany) and prepared according to our previously established protocols [9], [11] at 0-2 °C in a high sucrose perfusate. Next, hippocampal slices were incubated for 45 min at 32°C and then allowed to recover for at least one hour at room temperature before being used for recordings.

C. Experimental Conditions for SWR Induction

Slices were positioned on the HD-MEA chip (Fig.1b) and secured using a platinum harp. SWRs were recorded following a previously established protocol [11] under the following conditions: i) Spontaneous SWRs – Naturally occurring events in hippocampal slices. ii) Electrically Evoked SWRs – Induced through a single-high-frequency pulse at 100 Hz over a 1-sec duration at the Schaffer collateral pathway using an external bipolar, platinum/iridium electrode (World Precision Instruments, Germany GmbH), while recording network response by HD-MEA. iii) Chemically Induced SWRs – Generated via 8.5mM of K^+/0.5mM Mg^{2+}, and 100 µM 4-aminopyridine (4-AP) application to increase excitability.

D. Data Analysis

Custom Python scripts were used for data processing and event detection [8]. A hard-threshold algorithm and a fourth-order Butterworth filter (1–100 Hz) were applied for denoising local field potential (LFP) signals. Detected events were categorized into θ (5–12 Hz), β (13–35 Hz), γ (35–100 Hz), , SWR (120–240 Hz), and multi-unit spiking activity (MUA, 300–1000 Hz). Spectrograms were generated to illustrate frequency-time dynamics. To examine firing patterns, extracellular recordings were performed at a 14 kHz sampling frequency per electrode and a 1 Hz recording frequency to capture slow oscillatory brainwaves. Brain slice structures were imaged using a customized Stereomicroscope (Leica Microsystems, Germany) to use offline analysis to map tissue arrangement relative to extracellular recordings. All statistical analyses were performed with Originlab 2024. Differences between groups were examined for statistical significance using one-way analysis of variance (ANOVA) followed by Tukey's posthoc testing $P < 0.05$ was considered significant.

E. Mean Activity Analysis

Analyzed three selected parameters to describe the mean activity features of large-scale spatiotemporal LFP oscillations, including signal amplitude, LFP rate, and duration. The signal amplitude analysis was obtained through full-wave rectification and low-pass filtering with a cut-off frequency of 100 Hz. LFP rate was defined as the number of detected LFP events per minute and the duration was defined as the average time interval between the onset and offset of a single LFP event.

III. Results and Discussion

Recording and Network-level Analysis of CA3 Oscillations Using HD-MEA

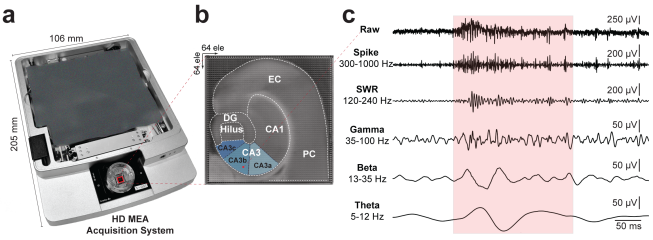

Figure 1. HD-MEA acquisition system (a), hippocampal slice on HD-MEA with CA3 subregions labeled (b), and representative waveforms of raw signal, MUA, SWRs, and slow oscillations (theta, beta, gamma) from CA3 (c).

HD-MEA recordings enabled precise identification and classification of oscillatory activity across the CA3 subregions (CA3a, CA3b, and CA3c) [12], capturing spontaneous and experimentally induced network dynamics with high spatiotemporal resolution (Fig. 1). Fig. 1a illustrates the HD-MEA acquisition system, which allows for large-scale electrophysiological recordings across thousands of electrodes, providing an unprecedented view of hippocampal activity. Fig. 1b displays a hippocampal slice positioned on the HD-MEA, with CA3 subregions clearly identified, enabling targeted spatial mapping of SWR propagation and neuronal activity patterns. This anatomical segmentation is critical for assessing regional differences in oscillatory events, as CA3b serves as the primary site of SWR initiation, with subsequent propagation toward CA3a and CA3c before reaching CA1. Fig. 1c presents exemplary waveforms extracted from CA3, demonstrating the diversity of oscillatory components recorded via HD-MEA. The raw signal captures all ongoing network activity, while multi-unit activity (MUA) highlights spiking patterns from neuronal ensembles. SWRs (~120–240 Hz) exhibit distinct high-frequency characteristics, distinguishing them from slower oscillations, including theta (5–12 Hz), beta (13–35 Hz), and gamma (35–100 Hz), which play complementary roles in hippocampal computation. This multi-band decomposition enables a comprehensive assessment of how different frequency components interact within CA3 circuits under various experimental conditions. Together, these results demonstrate how HD-MEA technology allows for high-resolution, network-wide analysis of CA3 oscillations, resolving the spatial origins, frequency composition, and propagation of SWRs with unmatched precision.

Frequency-Resolved Analysis of CA3 Oscillatory Activity

To systematically compare the spectral composition of CA3 oscillatory activity under spontaneous, electrically evoked, and pharmacologically induced (high K^+ / low Mg^{2+}, 4-AP) conditions, we analyzed raw signals alongside their decomposed frequency components, including multi-unit activity (MUA), SWRs (120–250 Hz), and "SOA" slow oscillatory activity (1–100 Hz) (Fig. 2, a-d). Spontaneous SWRs exhibited robust activity across MUA, SWR, and SOA spectra, indicating strong network recruitment and intrinsic

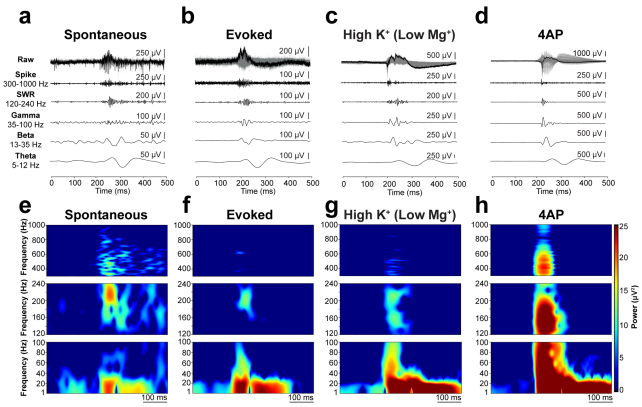

Figure 2. Waveforms (a-d) and spectral analysis (e-h) of CA3 activity across conditions: spontaneous, electrically evoked, high K^+ / low Mg^{2+}, and 4-AP-induced. MUA, SWR, and SOA power spectra highlight distinct oscillatory signatures and network recruitment patterns.

generation of high-frequency events (Fig. 2e). Electrically evoked SWRs showed reduced MUA and SWR amplitudes, and enhanced SOA, suggesting that external stimulation synchronizes network activity but fails to fully engage excitatory ensembles (Fig. 2f). In the high K^+ / low Mg^{2+} condition, MUA remained diminished, but SWRs and SOA were stronger than in the electrically evoked state yet weaker than spontaneous activity, reflecting a state of increased excitability without direct spike-driven recruitment (Fig. 2g). 4-AP-induced activity exhibited the highest power across all spectra, including MUA, SWR, and SOA, consistent with hyperexcitable network states due to K^+ channel blockade, leading to excessive firing and prolonged oscillatory bursts (Fig. 2h). Duration analysis revealed that spontaneous SWRs were the shortest (50-100 ms), with electrically evoked events slightly longer due to artificial network entrainment. High K^+ extended SWR duration, and 4-AP-induced oscillations were the longest (>250 ms), highlighting excessive excitatory drive and disrupted inhibitory control. These findings demonstrate how different induction methods uniquely shape CA3 oscillatory properties, providing a direct comparison of their effects on hippocampal network dynamics.

To complement the spectral and waveform analyses, we quantified key network activity metrics in the CA3 region across the four recording conditions. The number of active electrodes, LFP amplitude, event duration, and LFP rate were analyzed to assess the extent of network recruitment and oscillatory modulation (Fig. 3). Active electrode count (Fig. 3a) was highest in 4-AP and high K^+ / low Mg^{2+} conditions, reflecting broader network activation. Electrically evoked SWRs showed moderate recruitment, while spontaneous events engaged the fewest electrodes, indicating localized activation. Amplitude analysis (Fig. 3b) showed that spontaneous and electrically evoked SWRs had the lowest values. High K^+ increased amplitude significantly, while 4-AP exceeded spontaneous and other condition levels, highlighting its role in hyperexcitable states. Duration measurements (Fig. 3c) revealed that spontaneous SWRs were the shortest, while 4-AP-induced events were the longest, reflecting prolonged excitation. High K^+ extended SWR duration, whereas electrically evoked events remained brief. LFP rate (Fig. 3d) followed the same trend, with 4-AP showing the highest

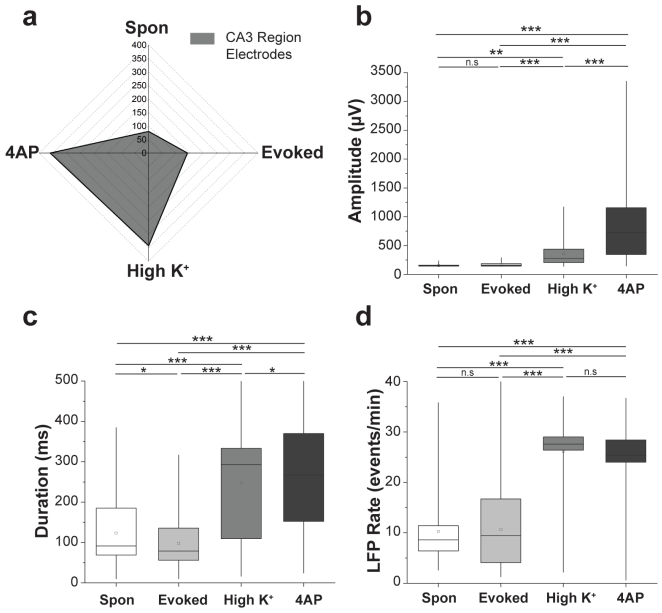

Figure 3. Quantification of CA3 oscillatory activity across conditions: number of active electrodes (a), LFP amplitude (b), event duration (c), and LFP rate (d), highlighting distinct network engagement patterns. (*p < 0.05, ANOVA) (b-d).

frequency, followed by high K^+, spontaneous, and evoked conditions, confirming that pharmacological manipulations significantly alter CA3 network dynamics. These results reinforce spectral and waveform analyses, demonstrating that 4-AP strongly enhances all oscillatory parameters, while high K^+ increases SWR activity without excessive firing. Electrically evoked SWRs engage the smallest network footprint, underscoring the differences in how each method modulates hippocampal activity.

Network-Wide Propagation and Spatiotemporal Mapping of SWR Activity

To examine the spatial distribution and propagation of SWRs across hippocampal subregions, we mapped LFP activity onto the hippocampal slice layout and analyzed spatiotemporal activation patterns in CA3a, CA3b, CA3c, and CA1 under spontaneous, electrically evoked, high K^+ / low Mg^{2+}, and 4-AP conditions (Fig. 4).

Topographical representations of SWR activity (Fig. 4, a–d) revealed distinct propagation patterns. Spontaneous SWRs originated predominantly in CA3b and propagated toward CA3a with limited spread to CA1, maintaining a localized yet structured trajectory. Electrically evoked SWRs showed sparse activation, primarily between CA3b and CA3a, with weak propagation into CA1, indicating limited network recruitment. In contrast, high K^+ / low Mg^{2+} conditions broadened SWR distribution, engaging CA3a, CA3b, and occasionally CA1, suggesting enhanced excitability but incomplete network synchronization. 4-AP-induced SWRs exhibited the most widespread activation, recruiting all CA3 subregions and excessively propagating into CA1, consistent with strong excitatory drive observed in spectral and statistical analyses. Spatiotemporal activation maps (Fig. 4, e–h) further highlighted differences in network-wide SWR propagation. Spontaneous SWRs followed a structured trajectory from CA3b to CA3a, whereas electrically evoked SWRs had a

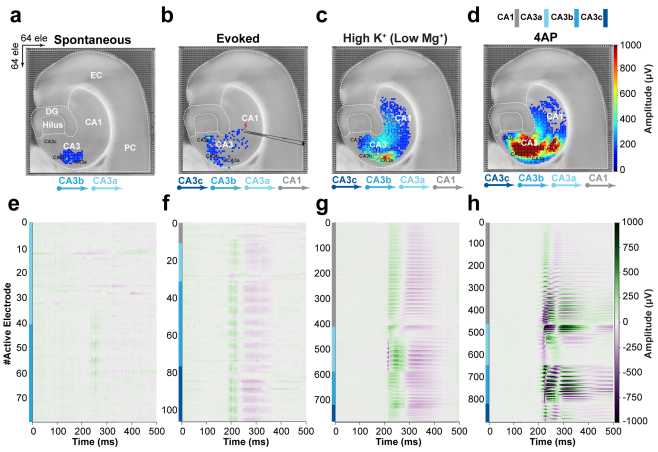

Figure 4: Topographical (a–d) and spatiotemporal (e–h) mapping of SWR activity across CA3 subregions and CA1 under spontaneous, electrically evoked, high K^+ / low Mg^{2+}, and 4-AP conditions, highlighting distinct propagation patterns and network recruitment.

weaker and sparser propagation pattern, extending from CA3c toward CA3b and CA3a, with minimal activity in CA1. High K^+ increased CA3 engagement and produced stronger propagation into CA1, suggesting heightened excitability and facilitating broader network recruitment. 4-AP, however, induced rapid and widespread activation, extending across CA3a, CA3b, CA3c, and CA1, indicating prolonged excitation and network-wide synchronization.

These results demonstrate that SWR propagation is highly dependent on the induction method. Spontaneous SWRs exhibit controlled, localized spread, while electrically evoked events show weak recruitment. High K^+ extends activity propagation, but only 4-AP drives full network-wide activation, likely due to prolonged excitatory bursts and reduced inhibitory control. The ability of HD-MEA to resolve these propagation dynamics with anatomical precision highlights its power in assessing large-scale hippocampal oscillatory activity, providing crucial insights into how different manipulations influence network-wide SWR engagement.

IV. Conclusion

This study provides a comprehensive, large-scale analysis of SWR generation and propagation in the CA3 region using HD-MEA. By directly comparing spontaneous, electrically evoked, and pharmacologically induced (high K^+ / low Mg^{2+}, 4-AP) SWRs, we reveal clear distinctions in network recruitment, oscillatory properties, and propagation dynamics across different induction methods. Spontaneous SWRs followed a structured propagation pattern, originating in CA3b and extending toward CA3a with a well-defined frequency profile across MUA, SWR, and SOA bands. Electrically evoked SWRs engaged the smallest network footprint, lacking MUA and showing weak propagation, suggesting limited recruitment of intrinsic circuit mechanisms. High K^+ increased SWR amplitude and extended propagation into CA1, while 4-AP induced excessive network-wide activation, elevating all spectral components and producing the longest-duration events due to heightened excitability. These findings demonstrate that SWR induction methods significantly shape network engagement, with pharmacological manipulations amplifying excitatory drive, while electrical stimulation fails to fully replicate physiological SWR dynamics. HD-MEA technology proves essential in capturing these differences, offering unparalleled resolution of hippocampal oscillations at both spatial and temporal scales. By establishing a quantitative framework for SWR characterization, this work advances our understanding of how hippocampal circuits generate and regulate oscillatory activity, with direct implications for neural computation, memory consolidation, and translational applications in cognitive and neuromodulatory therapies.

Acknowledgment

We would like to acknowledge the platform for behavioral animal testing at the DZNE-Dresden for their support.

References

[1] R. J. Dolan, “Emotion, Cognition, and Behavior,” vol. 298, no. November, pp. 1191–1195, 2002.

[2] J. Lisman, G. Buzsáki, H. Eichenbaum, L. Nadel, C. Ranganath, and A. D. Redish, “Viewpoints: how the hippocampus contributes to memory, navigation and cognition,” *Nat Neurosci*, vol. 20, no. 11, pp. 1434–1447, 2017.

[3] G. Buzsáki, “Hippocampal sharp wave-ripple: A cognitive biomarker for episodic memory and planning,” *Hippocampus*, vol. 25, no. 10, pp. 1073–1188, 2015.

[4] M. V. Sanchez-Vives, “Origin and dynamics of cortical slow oscillations,” *Current Opinion in Physiology*, vol. 15, no. Figure 1, pp. 217–223, 2020.

[5] H. Amin, “Balancing memory in sleep : firing barrages as a circuit breaker for reactivation,” *Signal Transduct Target Ther*, no. November, pp. 2–4, 2024.

[6] J. F. Ramirez-Villegas, N. K. Logothetis, and M. Besserve, “Diversity of sharp-wave-ripple LFP signatures reveals differentiated brain-wide dynamical events,” *Proc Natl Acad Sci U S A*, vol. 112, no. 46, pp. E6379–E6387, 2015.

[7] M. R. Karlócai *et al.*, “Physiological sharp wave-ripples and interictal events in vitro: What’s the difference?,” *Brain*, vol. 137, no. 2, pp. 463–485, 2014.

[8] X. Hu, B. A. Emery, S. Khanzada, and H. Amin, “DENOISING : Dynamic enhancement and noise overcoming in multimodal neural observations via high-density CMOS-based biosensors,” *Front Bioeng Biotechnol*, no. September, pp. 1–11, 2024.

[9] B. A. Emery, X. Hu, S. Khanzada, G. Kempermann, and H. Amin, “High-resolution CMOS-based biosensor for assessing hippocampal circuit dynamics in experience-dependent plasticity,” *Biosens Bioelectron*, vol. 237, no. May, p. 115471, 2023.

[10] X. Hu, S. Khanzada, D. Klütsch, F. Calegari, and H. Amin, “Implementation of biohybrid olfactory bulb on a high-density CMOS-chip to reveal large-scale spatiotemporal circuit information,” *Biosens Bioelectron*, vol. 198, no. March 2021, p. 113834, 2022.

[11] B. A. Emery, S. Khanzada, X. Hu, D. Klütsch, and H. Amin, “Recording and Analyzing Multimodal Large-Scale Neuronal Ensemble Dynamics on CMOS-Integrated High- Density Microelectrode Array,” *J. Vis. Exp.*, vol. 205, no. March, 2024.

[12] H. E. Scharfman, “The CA3 ‘backprojection’ to the dentate gyrus,” *Prog Brain Res*, vol. 163, no. 07, pp. 627–637, 2007.